Preprint
UCRL-JC-137593

Making Nanostructured Pyrotechnics in a Beaker

A.E. Gash, R.L. Simpson, T.M. Tillotson, J.H. Satcher, L.W. Hrubesh

This article was submitted to
International Pyrotechnics Seminars, Grand Junction, CO
July 17-21, 2000

April 10, 2000

U.S. Department of Energy
Lawrence Livermore National Laboratory

Making Nanostructured Pyrotechnics in a Beaker

A.E. Gash, R.L. Simpson*, T.M. Tillotson, J.H. Satcher and L.W. Hrubesh
Energetic Materials Center
Lawrence Livermore National Laboratory
Livermore, CA 94550

Abstract

Controlling composition at the nanometer scale is well known to alter material properties in sometimes highly desirable and dramatic ways. In the field of energetic materials component distributions, particle size, and morphology, effect both sensitivity and reactivity performance. To date nanostructured energetic materials are largely unknowns with the exception of nanometer-sized reactive powders now being produced at a number of laboratories. We have invented a new method of making nanostructured energetic materials, specifically explosives, propellants, and pyrotechnics, using sol-gel chemistry.[1-4] The ease of this synthetic approach along with the inexpensive, stable, and benign nature of the metal precursors and solvents permit large-scale syntheses to be carried out. This approach can be accomplished using low cost processing methods. We will describe here, for the first time, this new synthetic route for producing metal-oxide-based pyrotechnics. The procedure employs the use of stable and inexpensive hydrated-metal inorganic salts and environmentally friendly solvents such as water and ethanol. The synthesis is straightforward and involves the dissolution the metal salt in a solvent followed by the addition of an epoxide, which induces gel formation in a timely manner. Experimental evidence suggests that the epoxide acts as an irreversible proton scavenger that induces the hydrated-metal species to undergo hydrolysis and condensation to form a sol that undergoes further condensation to form a metal-oxide nanostructured gel. Both critical point and atmospheric drying have been employed to produce monolithic aerogels and xerogels, respectively. Using this method we have synthesized metal-oxide nanostructured materials using Fe^{3+}, Cr^{3+}, Al^{3+}, Ga^{3+}, In^{3+}, Hf^{4+}, $Sn^{4+}$and Zr^{4+} inorganic salts. Using related methods we have made nanostructured oxides of Mo, Ti, V, Co, Ni, Cu, Y, Ta, W, Pb, B, Pr, Er, Nd and Si. These materials have been characterized using optical and electron microscopy, infrared spectroscopy, surface area, pore size, and pore volume analyses.

The epoxide addition sol-gel technique is amenable the addition of insoluble materials (e.g., metals or polymers) to the viscous sol, just before gelation, to produce a uniformly distributed and energetic nanocomposite upon gelation. As an example energetic nanocomposites of Fe_xO_y and metallic aluminum are easily synthesized. The compositions are stable, safe and can be readily ignited. Production and characterization data of these novel energetic materials will be presented.

Introduction

The reactive properties of energetic materials are strongly affected by their micro and mesoscopic morphology. Many physical properties may be enhanced in materials called "nanocomposites", which are made from nanometer-scale building blocks of at least one of the composite materials. Sol-gel chemistry is an approach to creating structures at the nanometer scale and enables the formation of pyrotechnics in an entirely new way. Our main interest in the sol-gel approach to pyrotechnic materials is that it offers the possibility to precisely control the composition, morphology and reactivity of the target material at the nanometer scale. These are important variables for both safety and performance considerations. Those variables are difficult to achieve by other conventional techniques. Such control of the nanostructure could enable the creation of pyrotechnics with exceptional properties.

Sol-gel chemistry uses the hydrolysis and condensation of molecular chemical precursors, in solution, to produce nanometer-sized primary particles, called "sols".[5] Through further condensation the "sols" are linked to form a three-dimensional solid network, referred to as a "gel", with the solvent liquid present in its pores. A schematic representation of an iron oxide gel is shown in Figure 1. Evaporation of the liquid phase results in a dense porous solid referred to as a "xerogel". Supercritical extraction of the pore liquid eliminates the surface tension of the retreating liquid phase and results in highly porous lightweight solids called, "aerogels". These materials are uniform to the scale of a few nanometers. Therefore, sol-gel chemical routes are very attractive because they offer low temperature routes to synthesize homogeneous materials with variable compositions, morphologies, and densities.

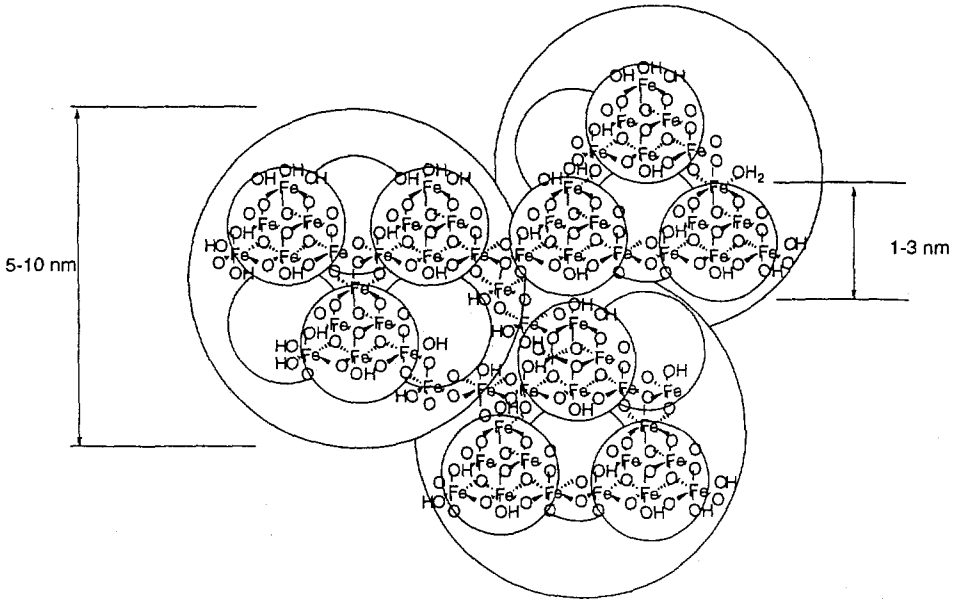

Figure 1. General representation of the primary particles and larger clusters made up of primary particles of a Fe_xO_y gel.

Nanostructured composites are multicomponent materials in which at least one of the component phases has one or more dimensions (length, width, or thickness) in the nanometer size range, defined as 1 to 100 nm.[6] *Energetic nanocomposites* are a class of material that have both a fuel and oxidizer component intimately mixed and where at least one of the component phases meets the size definition. A sol-gel derived pyrotechnic is an example of an energetic nanocomposite, in which metal-oxide nanoparticles react with metals and or other fuels in very exothermic reactions. The fuel resides within the pores of the solid matrix while the oxidizer comprises at least a portion of the skeletal matrix. Nanometer to millimeter size materials can be added to the matrix and processed to form a xerogel to achieve the desired performance properties. The sol-gel formulations, reported here, allow for intimate mixing of components at the nanoscale level and have the potential for water processing. The sol-gel methodology could also be used to make gels with potentially superior performance than existing formulations, and incorporate all the safety and low toxicity considerations of water or other environmentally acceptable processing solvent-based systems.

Experimental

Preparation of Fe_xO_y gels from inorganic Fe(III) salts. Ferric nitrate nonahydrate, $Fe(NO_3)_3 \cdot 9H_2O$, ferric chloride hexahydrate, $FeCl_3 \cdot 6H_2O$, ferric chloride, $FeCl_3$, and propylene oxide (99%) were used as received. Distilled water, 100% ethanol, and reagent grade methanol, 1-propanol, *t*-butanol, and acetone were also used. All syntheses were performed under room conditions of temperature and atmosphere. In a typical experiment, 0.65 g of $Fe(NO_3)_3 \cdot 9H_2O$ (1.6 mmol) was dissolved in 2.5 mL of 100% ethanol to give a clear red/orange solution that remained unchanged upon storage, for several months. If, instead, a 1.0 g portion of propylene oxide (17 mmol) was added the solution rapidly (~1 min.) turned dark red in color. This color change was accompanied by an exothermic release, as the vial became warm to the touch. This exothermic reaction was then followed by the formation of a monolithic dark red-brown opaque gel. The whole sequence of events (from epoxide addition to gelation) occurs within a time as short as 20 seconds to as long as six hours, depending on synthetic conditions. Similar methods have been employed by us and others to make lanthanide oxide and mixed silica-alumina gels, respectively.[7,8]

It is instructive to note how we defined and determined both the gelation point and the Fe_xO_y stoichiometry. All of the attempted syntheses were performed in glass vials so we could visually observe the flow of the reaction mixtures until the onset of gelation. We have qualitatively defined the gel point to be that at which the solution does not flow under the influence of gravity. We represent the stoichiometry of the iron-oxide gels as Fe_xO_y because, as of now, we do not know the exact oxidation state(s) of the iron in the material. We believe that it is Fe(III), however, in the absence of sound oxidation state characterization we feel it most prudent to represent the general stoichiometry as such. In addition, it is most probable that the iron-oxide gel contains significant amounts of both water and or hydroxyl groups. For simplicity, we have omitted recognizing these constituents with our abbreviated stoichiometry. We are currently attempting to

determine the true iron oxidation state(s) and the stoichiometric amounts of H_2O and hydroxyl groups in the material, results of which will be presented elsewhere.

Processing of Fe_xO_y gels. Aerogel samples were processed in a Polaron™ supercritical point drier. The solvent liquid in the pores of the wet gel was exchanged for $CO_2(l)$for several days. Then the temperature of the vessel was ramped up to ~45°C, while maintaining a pressure of ~100 bars. The vessel was then depressurized at a rate of about 7 bars per hour. Xerogel samples were processed by allowing them to dry under room conditions for various lengths of time.

Preparation of Fe_xO_y/Al(s) pyrotechnic nanocomposites. To prepare a Fe_xO_y/Al(*s*) pyrotechnic nanocomposite a stirred solution of Fe(III) salt was carefully monitored after the addition of propylene oxide. Just before gelation the viscosity of the solution increases rapidly. At the onset of the viscosity increase in the mixture, a weighed portion of Al(*s*) powder (diameter ~6 μm) was added to the stirring solution. The stirring permitted a relatively uniform distribution of the Al(*s*) in the metal-oxide gel matrix. The high viscosity of the solution prevented the Al(*s*) powder from settling to the bottom of the reaction vessel. Just prior to gelation the stir bar was removed from the slurrylike mixture. Samples prepared by this method were subjected to the same drying conditions as described above for processing to aerogels or to xerogel monoliths.

Physical characterization of Fe_xO_y aerogels and xerogels. Fourier transform-infrared (FTIR) spectra were collected on pressed pellets containing KBr (IR-grade) and a small amount of solid sample. The spectra were collected with a Polaris™ FTIR spectrometer. Surface area and pore volume and size analyses were performed by BET(Brunauer-Emmet-Teller) methods using an ASAP 2000 Surface Area Analyzer (Micromeritics Instrument Corporation). Samples of approximately 0.1-0.2 g were heated to 200°C under vacuum (10^{-5} Torr) for at least 24 hours to remove all adsorbed species. Nitrogen adsorption data was taken at five relative pressures from 0.05 to 0.20 at 77K, to calculate the surface area by BET theory.[9] High resolution transmission electron microscopy (HRTEM) was performed on a Philips CM300FEG operating at 300KeV using zero loss energy filtering with a Gatan energy Imaging Filter (GIF) to remove inelastic scattering. The images where taken under bright field conditions and slightly defocused to increase contrast. The images were also recorded on a 2K x 2K CCD camera attached to the GIF.

Results and Discussion

Gel formation studies. Table 1 is a summary of the results from various synthetic attempts used to fabricate Fe_xO_y gels. Examination of Table 1 reveals several synthetic combinations that resulted in the formation of mechanically strong, red-brown monolithic Fe_xO_y gels. There are some interesting observations documented in Table 1 that warrant further discussion. For instance, Fe_xO_y gels can be made using all three Fe(III) inorganic precursor salts used ($Fe(NO_3)_3 \cdot 9H_2O$, $FeCl_3 \cdot 6H_2O$, and $FeCl_3$). These salts are relatively inexpensive, easy to obtain, and can be stored without the need for an inert atmosphere. In addition, all of the synthetic transformations reported in Table 1 were performed under ambient conditions in simple and inexpensive glassware such as beakers. It is also

worthwhile to note that the Fe_xO_y gels can be prepared in benign polar protic solvents such as water or alcohols. Current large-scale production of some pyrotechnics require the use of toxic, flammable, and carcinogenic solvents like acetone, hexane, and hexachlorobenzene.[10] This aspect of the process presented here could result in cleaner and safer large-scale pyrotechnic production. Interestingly, all attempts to produce the Fe_xO_y gels in polar aprotic solvents, such as tetrahydrofuran or acetone, were unsuccessful.

Table 1. Summary of synthetic conditions for the synthesis of Fe_xO_y gels.

Precursor salt	Solvent	H_2O/Fe	Gel formation	t_{gel} (minutes)
$Fe(NO_3)_3 \cdot 9H_2O$	water	58	no	-
$Fe(NO_3)_3 \cdot 9H_2O$	methanol	9	no	-
$Fe(NO_3)_3 \cdot 9H_2O$	ethanol	9	yes	8
$Fe(NO_3)_3 \cdot 9H_2O$	1-propanol	9	yes	3.5
$Fe(NO_3)_3 \cdot 9H_2O$	*t*-butanol	9	yes	2
$FeCl_3 \cdot 6H_2O$	water	55	yes	3
$FeCl_3 \cdot 6H_2O$	acetone	6	no	-[(a)]
$FeCl_3 \cdot 6H_2O$	methanol	6	yes	23
$FeCl_3 \cdot 6H_2O$	methanol	9	yes	6.5
$FeCl_3 \cdot 6H_2O$	ethanol	6	yes	25
$FeCl_3 \cdot 6H_2O$	ethanol	9	yes	10
$FeCl_3 \cdot 6H_2O$	1-propanol	6	yes	60
$FeCl_3 \cdot 6H_2O$	1-propanol	9	yes	6
$FeCl_3 \cdot 6H_2O$	*t*-butanol	6	no	-[(b)]
$FeCl_3$	water	49	yes	2
$FeCl_3$	ethanol	0	No	-
$FeCl_3$	ethanol	9	yes	5

a. Dissolution of $Fe(NO_3)_3 \cdot 9H_2O$ in acetone is rapidly followed by precipitation of a yellow/brown solid.
b. In this case a brown precipitate was formed after addition of the propylene oxide.

Inspection of Table 1 shows that water (present as either waters of hydration of the respective precursor salt or as the solvent) was a necessary component in all of the successful syntheses. Attempted syntheses of Fe_xO_y gel from $FeCl_3$ in anhydrous ethanol resulted in indefinitely stable clear yellow/orange solutions. In a series of separate experiments, several portions of $FeCl_3$ were dissolved in ethanol with various amounts of added water. Identical amounts of propylene oxide were added to each mixture and the solutions were monitored for gel formation. Gel formation was observed in all of the vials where the mole ratio of H_2O/Fe was greater than 4. However, solutions where the

Fe/H_2O ratio was ≤4 were stable indefinitely. Some hydrolysis and condensation of Fe(III) had occurred in these solutions as they were dark red in color (characteristic color of oligomeric iron(III) oxide species)[11] however, it was not sufficient to bring about gel formation.

According to Table 1, the rate of gel formation appears to be faster for gels formed in alcoholic solvents (specifically ethanol and 1-propanol) using the $Fe(NO_3)_3 \cdot 9H_2O$ precursor as opposed to the $FeCl_3 \cdot 6H_2O$ salt. We believe that the difference in rates is due to the fact that there is more water (9 equivalents) present when the nitrate salt is used than when the hydrated chloride salt (6 equivalents) is used. To test this hypothesis we performed syntheses with the hydrated chloride salt in ethanol and 1-propanol where an additional 3 equivalents of water was added to each mixture (this made the total number of water equivalents 9). In both cases, the gel formation was significantly faster than when only 6 equivalents of water were present. The addition of water to the syntheses in ethanol and 1-propanol resulted in gel times of 10 and 6 minutes respectively. These numbers are essentially identical to those observed using the $Fe(NO_3)_3 \cdot 9H_2O$ precursor in those same solvents. Therefore, it appears that in alcoholic solvents the counterion does not appreciably affect the rate of gelation. However, the amount of water present does appear to affect the rate of gelation. This observation is not without precedence, as the rate of SiO_2 gel formation from silicon alkoxide precursors in alcoholic solvents has been shown to increase with increasing H_2O/Si ratio.[12]

Another synthetic parameter that was extensive investigated was the ratio of propylene oxide to Fe(III), denoted as Q. Several experiments were run where the Q was varied from 3-25 the results of which are shown in Table 2. One can see here that the rate of gel formation increases with Q. The dependence appears to be asymptotic, as there is relatively little difference (approximately a factor of 2) in the rate of gelation for syntheses where Q is 11 and 23 respectively. However, the difference between the rate of gelation for the two syntheses where Q is 7 and 6, respectively, is a factor of 1800. The data in Table 2 also indicate that there is a critical Q ratio (Q = ~6, under these conditions) below which no gel formation is observed, even after several months.

Table 2. Summary of the effect of propylene oxide/Fe mole ratio on the gel formation of Fe_xO_y gels made in ethanol from the precursor salt $Fe(NO_3)_3 \cdot 9H_2O$ ([Fe] = 0.37M).

Q Ratio: propylene oxide/Fe	Gel formation	Gel time (minutes)
3.4	no	-
5.0	no	-
6.0	yes	~7200
6.2	yes	~6000
7.0	yes	4.0
8.0	yes	2.5
8.6	yes	2.5
9.8	yes	2.0
11	yes	1.2

17	yes	0.90
21	yes	0.75
23	yes	0.63

Some of the Fe_xO_y gels described in Table 1 were dried under atmospheric conditions or supercritical conditions with $CO_2(l)$ to produce xerogel and aerogel monoliths respectively. Figure 2 contains photos of monolithic Fe_xO_y aerogel and xerogel samples. These photos indicate that monolithic Fe_xO_y aerogels and xerogels can be formed. Previous reports of sol-gel syntheses often resulted in the formation of powders of iron (III) oxide.[13,14] Here we demonstrate our ability to make monolithic porous iron (III) oxide using this synthetic approach. This particular aspect of our account cannot be understated. It allows the synthesis and shape casting of low-density porous iron-oxide materials, as well as those of pyrotechnic compositions, to make monolithic materials in a variety of shapes and sizes. This might eliminate the need for time-consuming, expensive, and potentially dangerous pressing and machining of the solids to make materials with precise sizes, densities, and geometries.

(a)

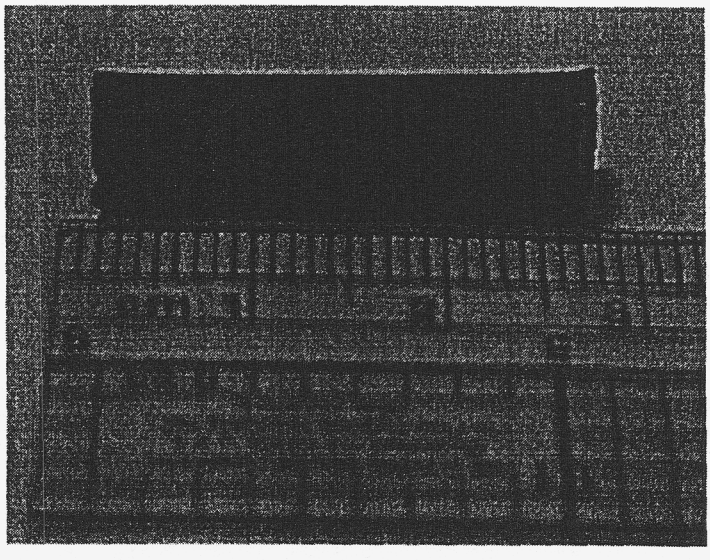

(b)

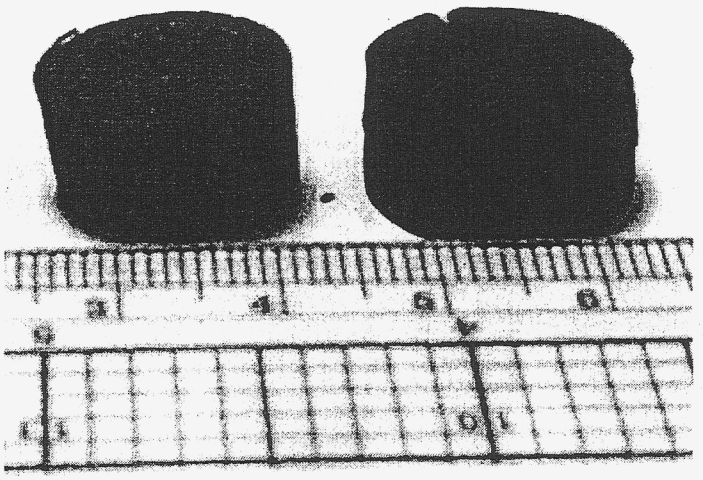

Figure 2 . Photographs of Fe_xO_y (a) xerogel (ρ = 0.85 g/cm^3) and (b) aerogel (ρ = 0.06 g/cm^3).

Morphology of Fe_xO_y gels. We utilized high-resolution transmission electron microscopy (HRTEM) to examine the morphology of Fe_xO_y aerogels. Figure 3 contains two micrographs of a Fe_xO_y aerogel. Figure 3a is a low magnification micrograph that reveals the expanded treelike structure of the aerogel. Qualitatively, the material appears to be a collection of clusters that contain cavities of mesoporous (20-50 nm) dimensions. The micrograph in Fig. 3b is of higher magnification than that in Fig. 3a and provides a fine representation of the size, shape, and connectivity of the clusters that make up the aerogel. It appears that these secondary particles are relatively uniform spheres with most having diameters in the 5-10 nm range. The particles appear to be connected to one another in clusters. These results clearly show that Fe_xO_y made by the epoxide-addition method is made up of nanometer-sized clusters. The observed Fe_xO_y aerogel microstructure is consistent with the generic sol-gel mechanism for gel formation.[5] According to that mechanism, the initial monomer (hydrated Fe(III) species in this case) polymerizes to form small oligomers (polymerization is probably due to the condensation of hydrated Fe(III) monomers).[15] These oligomers then undergo further growth until they begin to link together to form a sol. These clusters eventually link together to form an extended network throughout the medium that then rapidly thickens to form a gel.

(a)

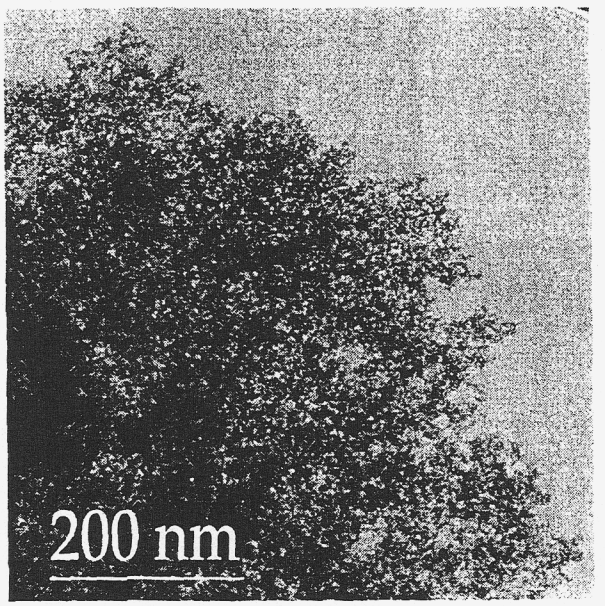

(b)

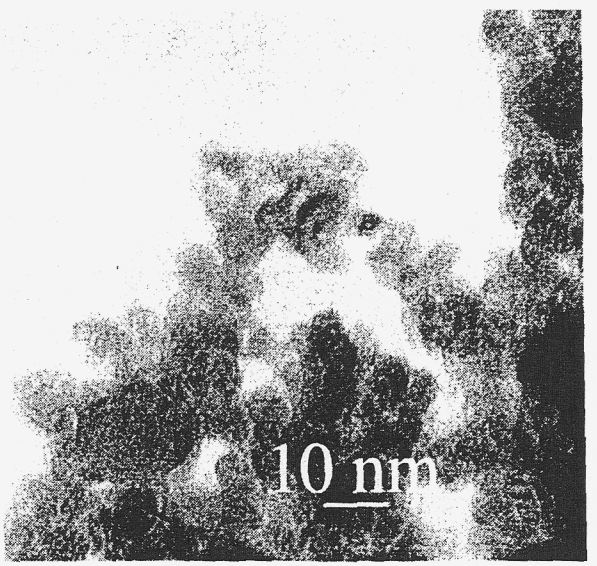

Figure 3. High-resolution transmission electron micrographs of Fe_xO_y aerogel at two different magnifications.

Synthesis of energetic nanocomposites. This sol-gel method allows for the addition of insoluble materials (e.g., metals or polymers) to the viscous sol, just before gelation, to produce a uniformly distributed and energetic nanocomposite upon gelation. Al metal (as a fine powder ~6 μm diameter) was added to some Fe_xO_y gel syntheses just before gelation to produce Fe_xO_y/Al(*s*) pyrotechnic nanocomposites. This same process

can be used with particle sizes from nanometers to millimeters and particle densities from low to high. These nanocomposites were subsequently processed to make both a xerogel and aerogel of the material. A photo of a sample of $Fe_xO_y/Al(s)$ aerogel is shown in Fig. 4. One can see the small shiny spheres of Al (6 μm) uniformly dispersed throughout the Fe_xO_y matrix. The pyrotechnic nanocomposite can be ignited using a propane torch. A photo of the ignition of one such nanocomposite is shown in Fig. 5.

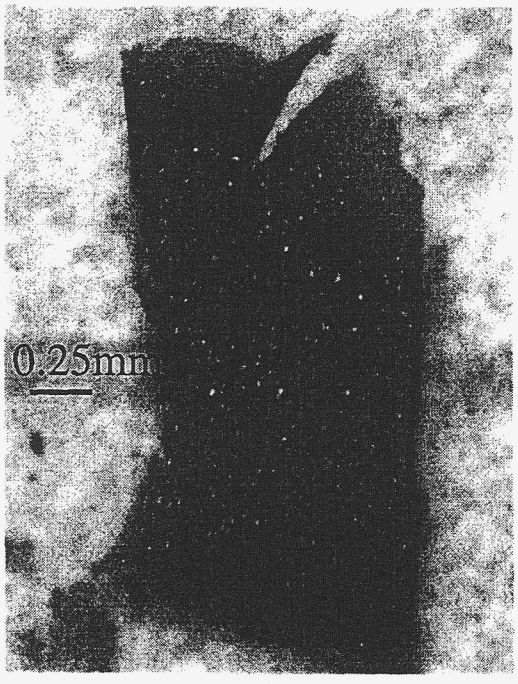

Figure 4. Photo of $Fe_xO_y/Al(s)$ aerogel under an optical microscope. Note the distribution of $Al(s)$ spheres.

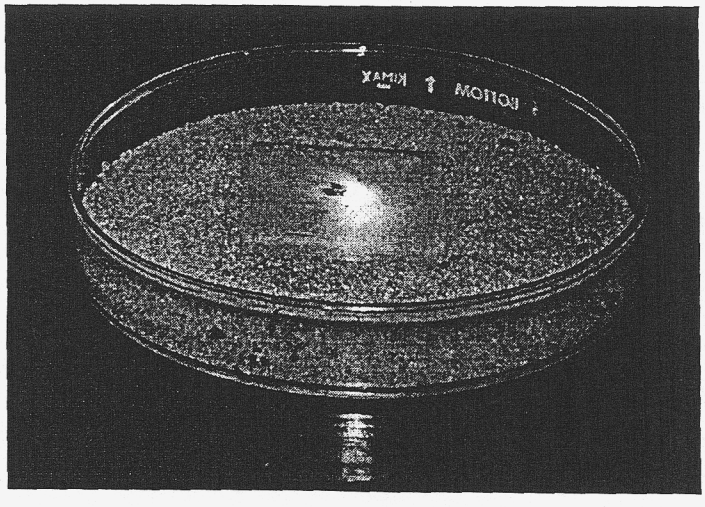

Figure 5. Photo of thermally ignited $Fe_xO_y/Al(s)$ nanocomposite.

The nature of the wet nanocomposites also affords an additional degree of safety. In our hands, the wet pyrotechnic nanocomposites cannot be ignited until the drying process is complete. This property should allow the production of a large quantity of the pyrotechnics that can be stored safely for some time and dried shortly before its use.

The sol-gel approach also allows the relatively simple incorporation of other metal oxides into the Fe_xO_y matrix to make a mixed-metal-oxide material.[16] Different metal-oxide precursors can be easily mixed into the Fe(III) solution, before the addition of the epoxide. Dilution of the thermitic material with inert oxides such as Al_2O_3 (from dissolved $AlCl_3$ salt) or SiO_2 (from added silicon alkoxide) leads to a pyrotechnic material that is not as energetic as a pure iron(III)-oxide-aluminum mixture. We have performed such syntheses. Qualitatively, the resulting pyrotechnics have noticeably slower burn rates and are less energetic. Alternatively, one could add metal-oxide components that are more reactive with Al(*s*) to increase the energy released.[17] Finally, this would also permit the addition of metal-oxide constituent(s) that provide a desired spectral emission to the energetic nanocomposite. This type of synthetic control should allow the chemist to tailor the pyrotechnic's burn and spectral properties to fit a desired application.

FTIR characterization of Fe-based gels. Figure 6 is and overlay of the FTIR spectra of the Fe_xO_y aerogel and its vacuum dried (200°C) product. The spectrum of the Fe_xO_y aerogel (Fig. 6a) contains many absorptions. The intense and broad absorption in the 3200-3600 cm^{-1} region likely corresponds to ν(O–H) stretching vibrations of adsorbed water (sample was synthesized, stored, and FTIR spectrum was taken under room conditions) and O–H moieties present in the solid. In addition, the absorption at ~1630 cm^{-1} is likely due to the bending mode of water $\delta(H_2O)$.[18] The presence of O–H groups in the IR of Fe_xO_y synthesized by solution methods is very common.[19] The absorptions present at 2800-3000 cm^{-1} are due to ν(C–H) vibrations. These, as well as the absorptions present from 1400-800 cm^{-1} are probably due to ethanol (solvent used), residual propylene oxide, or side products of the ring opening of the propylene oxide. The absorptions between 700 cm^{-1} and 500 cm^{-1} are those from the Fe–O linkages that make up the framework of the aerogel. All of the phases of iron oxides and oxyhydroxides have characteristic IR vibrations in this region.[19,20] The assignment of the spectrum shown in Fig. 6a to one particular phase of iron oxide is not straightforward. Notwithstanding, with the FTIR evidence shown here we tentatively conclude that the non-heat-treated Fe_xO_y aerogel material is probably an iron oxyhydroxide phase. We intend to further pursue the identification of the Fe_xO_y phase(s) present in this material through the use of powder x-ray diffraction (PXRD) and x-ray absorption fine structure spectroscopy (XAFS).

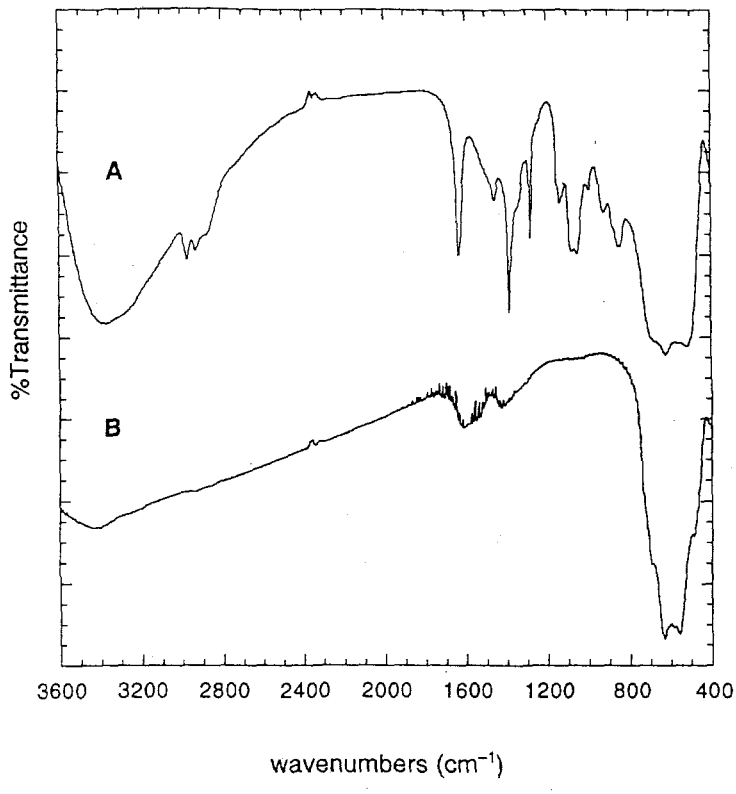

Figure 6. FT-IR spectra of a) Fe_xO_y aerogel and b) the same aerogel after heat treatment at 200°C under dynamic vacuum.

The spectrum shown in Fig. 6b is that of the Fe_xO_y aerogel that has been heated to 200°C under a dynamic vacuum. This heat treatment results in a mass loss of ~30% of the material. There are three notable differences between this spectrum and that of the Fe_xO_y aerogel. First, the absorption in the 3200-3600 cm^{-1} region of the spectrum is much less intense in the heat-treated sample. This is possibly due to the removal of a large percentage of the O–H moieties present in the original aerogel through condensation of two neighboring OH groups to give a single oxygen bridge. Second, there is no trace of the absorptions assigned to C–H bonds present in the heat-treated sample. These organic constituents have also been removed in the heating process. And finally, the two intense absorptions at 510 and 615 cm^{-1} in the original aerogel have shifted and split into three peaks at 565, 585, and 630 cm^{-1} respectively. The location of the IR bands present in the heat-treated sample match very well to those reported for maghemite, the γ-phase of Fe_2O_3.[20] It is worthwhile to note that maghemite is magnetic and that the heat-treated material in Fig. 6b is also magnetic.

Table 3 summarizes the surface areas, pore volumes, and average pore sizes for several Fe_xO_y aerogels and xerogels. Before discussing this data in detail we would like to make two issues clear. First, nitrogen adsorption surface area methods are known to only reliably measure the surface area of pores with mesoporic dimensions. Therefore, the surface areas of materials present in Table 3 do not take into account the contribution to the surface area of micro (<2 nm diameter) or macropores (>50 nm diameter).[9]

Second, the accuracy of pore volume and size measurements, by nitrogen adsorption methods, of aerogel materials have been questioned.[21] Therefore, we only intend to use this data for qualitative comparison of the Fe_xO_y materials to one another and not as absolute determinations.

In general, all of the materials listed in Table 3 have high surface areas and pore diameters whose dimensions are in the micro to lower mesoporic (2-20 nm) region. Note that the xerogel solid has a comparable total surface area to the aerogel material made under identical conditions. However, the pore volume and average pore diameter of the xerogel sample are significantly smaller than that of the aerogel sample (0.22 mL/g and 2.6 nm compared to 1.25 mL/g and 12 nm respectively). This is expected as the evaporation of the ethanol from the xerogel sample exerted substantial capillary forces on the gel's pore structure, which resulted in significant shrinkage of the pores, relative to the aerogel sample.

Table 3. Summary of properties of Fe_XO_y aerogels and xerogels.

Gel type [(a)]	Precursor salt	Solvent	Surface area (m^2/g)	Pore volume (mL/g)	Average pore diameter (nm)
Xero (200)	$Fe(NO_3)_3 \cdot 9H_2O$	ethanol	300	0.2	2.6
Aero (100)	$Fe(NO_3)_3 \cdot 9H_2O$	ethanol	560	1.8	11
Aero (200)	$Fe(NO_3)_3 \cdot 9H_2O$	ethanol	360	1.3	12
Aero (300)	$Fe(NO_3)_3 \cdot 9H_2O$	ethanol	190	1.0	19
Aero (200)	$Fe(NO_3)_3 \cdot 9H_2O$	1-propanol	460	1.8	12
Aero (200)	$FeCl_3 \cdot 6H_2O$	water	430	3.4	15
Aero (200)	$FeCl_3 \cdot 6H_2O$	methanol	410	3.3	23
Aero (200)	$FeCl_3 \cdot 6H_2O$	ethanol	480	4.6	23

a. The number in parentheses is the temperature in degrees Celsius that each respective gel was heated to under a dynamic vacuum to ensure removal of all adsorbed species before surface area analyses.

Several Fe_xO_y gels were heat-treated at three different temperatures prior to analyses (100, 200, and 300°C). As a result all three aerogels have notably distinct microstructural properties. The surface areas, and pore volumes decrease while the pore diameters increase with increasing drying temperature. This has been previously noted in studies of other metal-oxide aerogels.[22] The reasoning for these observations is as follows. According to the FTIR analyses there are many hydroxyl groups present in these materials. Certainly, many of the hydroxyls are surface bound and therefore, heating induces the condensation of the hydroxyl groups. This process has the effect of pulling together the small particles that make up the microstructure of the gel. As a result, these materials have reduced surface areas and pore volumes as well as enlarged pore sizes. Evidently, the extent of this process is more pronounced with increasing heating temperatures.

The aerogel made from the $FeCl_3 \cdot 6H_2O$ precursor has a considerably larger surface area, pore volume, and pore diameter than that made from the $Fe(NO_3)_3 \cdot 9H_2O$ precursor. Regardless, these results suggest that the surface areas and pore characteristics of the Fe_xO_y gels can be significantly altered by the choice of solvent, Fe(III) precursor, drying method, and post-synthesis heat treatment. This enables the chemist to have a certain measure of control over the materials properties, which may affect their performance as energetic nanocomposites.

Conclusions

In summary we have presented the invention of a class of nanostructured pyrotechnics that have new and potentially improved properties over conventional materials. We have utilized sol-gel chemistry to produce energetic nanocomposite of the general metal(1)-oxide oxidizer and metal(2) fuel, composition formula $M_{x(1)}O_y/M_{(2)}(s)$. Extensive analytical characterization presented has indicated that the material is made up of nanoscale building blocks. The sol-gel method is a safe, inexpensive, convenient, and flexible route to the synthesis of these types of nanocomposites. It is a suitable method to control the composition, morphology, and density of the final material, all of which can affect the energetic and performance properties of the resulting pyrotechnic. We are currently in the process of evaluating the performance properties of these new materials.

Acknowledgements

We would like to thank Dr. John Holtzrichter and Dr. Rokaya Al-Ayat for their support during the development of this effort. We would also like to acknowledge Mrs. Suzanne Hulsey and Mr. Mark Wall for their assistance and expertise in nitrogen adsorption and HRTEM analyses, respectively.

References

1) Tillotson, T. M.; Hrubesh, L. W.; Simpson, R. L.; Lee, R. S.; Swasinger, R. W.; Simpson, L. R. *J. Non-Cryst. Solids* **1998**, *225*, 358-363.

2) Simpson, R. L.; Swasinger, R. W.; Forbes, J. W.; Lee, R. S.; Cutting, J.; Tillotson, T. M.; Hrubesh, L. W. "New Formulations and Material Charcterization, Joint DoD/DOE Munitions technology Development Program FY99 Progress Report," UCRL-ID-103482-99, Lawrence Livermore National Laboratory, 1999.

3)Simpson, R. L.; Tillotson, T. M.; Hrubesh, L. W.; Gash, A. E., *Nanostructured Energetic Materials Derived from Sol-gel Chemistry*, Proccedings Institut Chemische Energetic Materials Analysis, Diagnostic, and Testing Meeting, Karlsruhe, Germany, June 27-30, 2000,

4)Simpson *et al.* Patents Pending, 2000.

5) Brinker, C. J.; Scherer, G. W. *Sol-Gel Science*; Academic Press, Inc.: Boston, 1990.

6) Dagani, R. *C&E News*, June 7, 1999 issue, **1999**, *77*, 25.

7) Tillotson, T. M.; Sunderland, W. E.; Thomas, I. M.; Hrubesh, L. W. *J. Sol-Gel Sci. Technol.* **1994**, *1*, 241.

8) Itoh, H.; Tabata, T.; Kokitsu, M.; Okazaki, N.; Imizu, Y.; Tada, A. *Journal of the Ceramic Society of Japan* **1993**, *101*, 1081-1083.

9) Gregg, S. J.; Sing, K. S. W. *Adsorption, Surface Area, and Porosity*; 2nd ed.; Academic Press: London, 1982.
10)Strategic Environmental Research and Development Program Home Page, *http://www.serdp.org*, Feb. 2000.
11) Flynn, C. M. *Chem. Rev.* **1984**, *84*, 31-41.
12) Gottari, V.; Gulielmi, M.; Bertoluzza, A.; Fagnano, C.; Morelli, M. A. *J. Non-Cryst Solids* **1984**, *63*, 71-80.
13) Wang, C.-T.; Willey, R. J. *J. Non-Cryst. Solids* **1998**, *225*, 173.
14) Liu, X. Q.; Tao, S. W.; Shen, Y. S. *Sensors and Actuators B* **1997**, *40*, 161.
15) Knight, R. J.; Sylva, R. N. *J. Inorg. Nucl. Chem.* **1974**, *36*, 591-597.
16) Livage, J.; Henry, M.; Sanchez, C. *Progress Solid St. Chem.* **1988**, *18*, 259.
17) Wang, L. L.; Munir, Z. A.; Maximov, Y. M. *J. Mater. Sci.* **1993**, *28*, 3693.
18) Nakamoto, K. *Infrared and Raman Spectra of Inorganic and Coordination Compounds*; 5th ed.; John Wiley and Sons, Inc.: New York, 1997.
19) Gehring, A. U.; Hofmeister, A. M. *Clays and Clay Minerals* **1994**, *42*, 409.
20) Music, S.; Gotic, M.; Popovic, S.; Czako-Nagy, I. *Mater. Lett.* **1994**, *20*, 143.
21) Scherer, G. W. *J. Non-Cryst. Solids* **1998**, *225*, 192-199.
22) Wu, N.-L.; Wang, S.-Y.; Rusakova, I. A. *Science* **1999**, *285*, 1375.

This work was performed under the auspices of the U.S. Department of Energy by the University of California, Lawrence Livermore National Laboratory under Contract No. W-7405-Eng-48.